

> REPLACE THIS LINE WITH YOUR MANUSCRIPT ID NUMBER (DOUBLE-CLICK HERE TO EDIT) <

High Performance Fiber Laser Resonator for Dual Band (C and L) Sensing

Arturo Sanchez-Gonzalez (<https://orcid.org/0000-0002-8877-2050>), Rosa Ana Perez-Herrera (<https://orcid.org/0000-0002-6856-9143>), Pablo Roldan-Varona (<https://orcid.org/0000-0002-4263-8243>), Luis Rodriguez-Cobo (<https://orcid.org/0000-0002-2068-2956>), Jose Miguel Lopez-Higuera (<https://orcid.org/0000-0002-8615-8487>), *Senior Member, IEEE*, and Manuel Lopez-Amo (<https://orcid.org/0000-0002-9399-5398>), *Senior Member, IEEE*

Abstract—This work presents an experimental analysis and comparison of the performance of quasi-randomly distributed reflectors inscribed into a single-mode fiber as a sensing mirror both in C- and L-band. Single-wavelength emission has been obtained in either band when using these artificially controlled backscattering fiber reflectors in a ring-cavity fiber laser. Single-longitudinal mode operation with an optical signal to noise ratio (OSNR) of 47 dB and an output power instability as low as 0.04 dB have been measured when employing a C-band optical amplifier. When replaced by an L-band optical amplifier, a single-longitudinal mode behavior has also been obtained, showing an OSNR of 44 dB and an output power instability of 0.09 dB. Regarding their performance as fiber-laser sensing systems, very similar temperature and strain sensitivities have been obtained in both bands, comparable to fiber Bragg grating sensors in the case of temperature and one order of magnitude higher in the case of strain variations.

Index Terms—artificially controlled backscattering reflectors, C-band, erbium-doped fiber laser, L-band, optical fiber sensor, single-longitudinal mode.

I. INTRODUCTION

FROM its first implementation in the 90's [1], optical fiber lasers for sensing applications have emerged as an appealing and continuously evolving technology. These lasers have different gain media and resonators, that comprise different kind of mirrors depending on the application. Both the classic and the more recent distributed mirror versions stand out for their electromagnetic interference immunity, chemical corrosion resistance, reliability over wide temperature ranges, and ability to multiplex a wide range of sensors along a single fiber or network [2]. Such is the interest generated that currently its application has spread to many areas with impact on the quality of human life such as surgery [3], seismography [4], medical imaging [5], and monitoring of ionizing radiation [6], among others.

This work is part of the project PID2019-107270RB, funded by MCIN/AEI/10.13039/501100011033 and FEDER “A way to make Europe”, the Ministerio de Educación, Cultura y Deporte of Spain (PhD grant FPU2018/02797), and PDC2021-121172, funded by MCIN/AEI/10.13039/501100011033 and European Union “Next generationEU”/PTR. (Corresponding author: Rosa Ana Perez-Herrera).

Arturo Sanchez-Gonzalez, Rosa Ana Perez-Herrera, and Manuel Lopez-Amo are with the Department of Electrical, Electronic and Communications Engineering, and Institute of Smart Cities (ISC), Public University of Navarra, 31006 Navarra, Spain (e-mail: arturo.sanchez@unavarra.es; rosa.perez@unavarra.es; mla@unavarra.es)

Focusing on the amplification medium of the sensing system, erbium-doped fiber-based lasers are one of the most widespread options. These lasers show high optical signal to noise ratios (OSNRs) as well as narrow emission lines. However, there is a notable downside in that the homogeneous gain broadening behavior of the erbium-doped fiber (EDF) cause the lasing to suffer from mode competition, mode hopping, and multimode oscillation [7], in cavities of certain length [8]. All of these end up resulting in considerably unstable laser emission that limits the performance of the laser when used in a sensing system.

Different techniques have been proposed to mitigate these problems, one of the most recent being the use of random distributed feedback lasers. These lasers have the distinctive feature of employing Rayleigh backscattering gathered along long fiber sections as distributed reflectors, achieving a mode-less behavior as well as high OSNR and power stability [9]. Moreover, their capability of being internally modulated without frequency restrictions [10] simplify the design of schemes for quasi-distributed fiber optic sensor multiplexing [11].

A more direct approach to cope with the instability challenge is to achieve single-longitudinal mode (SLM) behavior in the erbium doped fiber laser (EDFL) sensing system. Nevertheless, achieving this generally comes at the expense of a substantial increase in the cost and complexity of the cavity. For instance, using saturable absorbers implies the insertion of passive EDF sections in the resonator [12]; power equalization between lines must be guaranteed in self-injection lasers [13]; and the introduction of fiber Bragg gratings (FBGs) in combination with narrow phase-shifted FBGs (PS-FBGs) in the cavity hinders their use as a sensor system [14]. A solution that seems to be emerging at the moment is to assist the laser emission by means of reflectors in which the backscattering is artificially and pseudo-randomly increased along short fiber sections. This new structure, serving simultaneously as a mirror of the cavity

Pablo Roldan-Varona is with Photonics Engineering Group, University of Cantabria, 39005 Santander, Spain, and also with the Instituto de Investigacion Sanitaria Valdecilla (IDIVAL), 39011 Cantabria, Spain (e-mail: pablo.rolدان@unican.es).

Luis Rodriguez-Cobo is with CIBER-bbn, Instituto de Salud Carlos III, 28029 Madrid, Spain (e-mail: luis.rodriguez@unican.es).

Jose Miguel Lopez-Higuera is with Photonics Engineering Group, University of Cantabria, 39005 Santander, Spain, and CIBER-bbn, Instituto de Salud Carlos III, 28029 Madrid, Spain, and also with the Instituto de Investigacion Sanitaria Valdecilla (IDIVAL), 39011 Cantabria, Spain (e-mail: lopezhjm@unican.es).

> REPLACE THIS LINE WITH YOUR MANUSCRIPT ID NUMBER (DOUBLE-CLICK HERE TO EDIT) <

and as a sensor, tries to replicate the original physical phenomenon of random distributed feedback fiber lasers but without requiring long fiber spools as distributed reflectors. Although promising, recent studies have required artificially controlled backscattering fiber reflectors (ACBFRs) longer than two meters in length to achieve SLM behavior in laser sensing systems [15].

Finally, it is worth noting that the comparison of previous SLM techniques refers mainly to C-band, because in L-band the number of reported EDFL sensing systems is significantly short. Some examples can be found in [16][17][18]. This is due to the high cost of components compared to C-band, as well as the higher attenuation in the optical fiber due to the tails of the largely far-infrared absorption peaks [19]. This higher attenuation means that in L-band there is less demand of components for telecommunications networks, and therefore prices are higher than in C-band. However, this band is essential for sensing certain gases extremely important for both pollution monitoring and safety reasons, such as carbon dioxide and hydrogen sulfide [20]. Therefore, further efforts should be made in the L-band.

Trying to address the lack of L-band sensing fiber lasers as well as the complexity and cost of achieving SLM operation, in this work we propose a high performance ACBFR assisted fiber laser resonator for dual band (C and L) sensing. To the best of our knowledge, this is the first scheme that achieves highly-stable SLM operation by employing an ACBFR as short as 15 mm, reducing the previously reported case to less than 1 % in length [15]. Moreover, due to the pseudo-random nature of the designed reflector compared to the well-known FBGs, the resonator proposed in this work can be used to measure in different bands with comparable performance.

II. WORKING PRINCIPLE: INSCRIPTION PROCESS

The inscription of the single-mode fiber (SMF) was carried out by means of a commercial femtosecond Fiber Laser Chirped Pulse Amplifier (FLCPA; CALMAR Laser, Inc.) as the core element of the transversal inscription setup. Following the slit beam shaping technique [21], the pulses generated by the FLCPA pass through an iris diaphragm and adjustable slit before reaching the objective lens of the optical system. In this way, it is possible to fine tune the focal volume of the laser in order to ensure both a better control over the dimensions of each individual inscription and that refractive index changes are induced over the entire core cross-section of the fiber [21]. From this point, the objective lens with a numerical aperture of 0.42 (Mitutoyo Europe, GmbH) focuses the pulses on the Fiber Under Test (FUT) producing the refractive index change (RIC). The positioning and alignment of the sample is made possible by placing it on a high precision air-bearing XYZ stage (Aerotech, Inc.). Up to this point, the process resembles that of previous studies [22]. However, given that laser emission was now to be achieved both in C- and L-band simultaneously by a single ACBFR, the inscription parameters had to be revisited, widening their ranges of variation during the randomly modulated inscription. Particularly, a fast-changing pulse

energy of 0.19 to 0.9 μJ and a spatial period of 1 to 12 μm were selected, implying an increase in variability of 65 and 20 % respectively. Regarding pulse duration and operating wavelength, these remain imposed by the particular FLCPA employed at 370 fs and 1030 nm.

The randomness of the inscribed structure was achieved by randomly modulating the pulse repetition rate at every update (which corresponds to approximately 100 ms). Therefore, a quasi-random physically inscribed structure was achieved, with a varying envelope period of tenths of micrometers; the period was maintained for several tenths of micrometers and then randomly altered. Due to the repetition rate of the femtosecond laser could not be simultaneously modulated at the same rate as the pulse inscription speed, it was not possible to inscribe randomly. As an alternative, quasi-randomly spaced spots were achieved, with random variations in spatial periods between groups of pulses but a constant period within each envelope, as presented in [22].

Before evaluating the performance of this reflector into a ring-cavity fiber laser, its reflectance was characterized by means of an Optical Spectrum Analyzer (OSA; Anritsu MS9740A) with a spectral resolution of 0.03 nm. Fig. 1 illustrates the results and, as expected, a random reflectance under 5 % was measured throughout the entire spectral range under study.

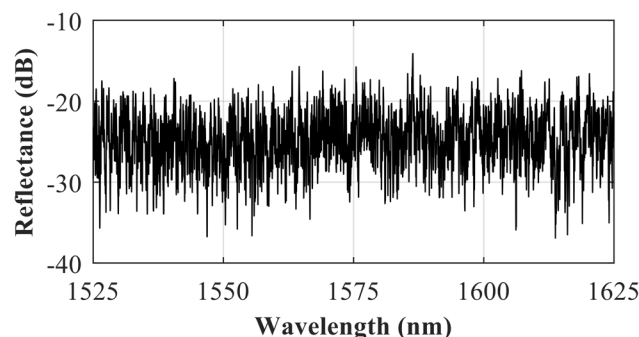


Fig. 1. Reflectance of the ACBFR in the C- and L-band spectral range.

Secondly, backscattered optical power along the length of the ACBFR was also analyzed by using an optical backscatter reflectometer (OBR; Luna OBR 4600) which achieves an ultra-high spatial resolution of 0.1 mm under its time-domain acquisition mode, as reported in [23]. It is noteworthy that the OBR employed performs the desired measurement over almost the entire spectral range under study (1545 to 1588 nm). The free termination of the ACBFR was immersed in index matching gel to avoid undesired reflections. As Fig. 2 shows, a backscattered light amplitude of about 55 dB over the noise floor was measured at the location of the ACBFR, at a distance of around 2.62 m from the OBR connector. The length of the inscription was approximately 15 mm.

> REPLACE THIS LINE WITH YOUR MANUSCRIPT ID NUMBER (DOUBLE-CLICK HERE TO EDIT) <

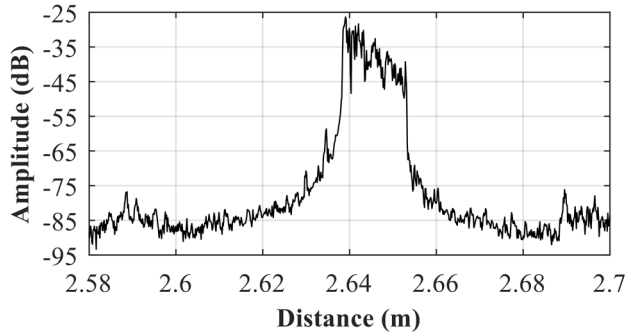


Fig. 2. Backscattered optical power as a function of fiber length for the ACBFR. The fiber sample was located about 2.62 m from the connector of the OBR.

III. EXPERIMENTAL SETUP

The schematic diagram of the experimental setup carried out to evaluate the laser generation and sensor properties when using these distributed reflectors within a ring-cavity fiber acting as a mirror is presented in Fig. 3. As it is illustrated, both C- and L-band lasers share the same cavity and components with the exception of the erbium doped fiber amplifier (EDFA), ensuring that the results obtained could be subsequently compared. In this configuration, the light injected into the cavity ends at a fiber loop mirror (FLM) after passing through ports 1 and 2 of the central optical circulator (CIR2). The FLM, at the right side of the structure, comprises another optical circulator (CIR3) in which ports 1 and 3 are connected to a variable optical attenuator (VOA). This mirror serves as a reflector of the resonator while allowing the fine tuning of its OSNR as well as lasing stability [15]. Once the recirculating signal reaches the third port of CIR2, it is guided through ports 1 and 2 of CIR1 to end at an optical coupler (OC). At this optical coupler, 5 % of the signal is decoupled to be monitored, while the remaining 95 % travels through a polarization controller (PC) to reach the quasi-distributed reflector of the cavity. This PC is also used to adjust the lasing stability, providing an intracavity mechanism for tuning the polarization state of the feedback light-wave as well as compensating for the slight polarization dependent gain [24]. Finally, the light reflected from the ACBFR recirculates through the PC, OC and ports 2 and 3 of CIR1, entering in the EDFA via its input port and closing the round trip along the cavity.

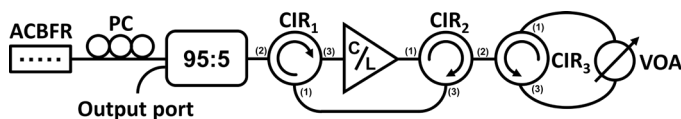


Fig. 3. Schematic diagram of the experimental ring-cavity fiber laser setup, wherein a micro-drilled optical fiber was used as a reflector. ACBFR: Artificially controlled backscattering fiber reflector. PC: polarization controller. CIR: Circulator. VOA: Variable optical attenuator.

With regard to the used EDFAs, two options were employed. One of them consists of a benchtop L-band EDFA commercial amplification unit (ManLight HWT-EDFA-B-SC-L30) for the L-band. The other one uses a 980/1550 nm wavelength division

multiplexer (WDM) that injected a pump laser optical power centered at 976 nm (Thorlabs PL980P330J). This power feeds 2.5 m of a highly erbium-doped fiber placed into the ring resonator for the C-band case. The chosen EDF that acts as gain medium was the I25 (Fibercore Inc.), characterized by a peak core absorption ranging from 7.7 to 9.4 dB/m at 1531 nm. The remaining 1550 nm port of the WDM corresponded to the input port of the C-band optical amplifier.

All the experimental measurements here presented were carried out at room temperature, without vibration isolation nor temperature compensation techniques employed.

IV. RESULTS AND DISCUSSION

A. C-band Laser Generation Properties

The enhancement in both laser emission and sensing applications using an ACBFR has already been discussed in previous works [25]. However, the inscription parameters originally designed for emission around 1550 nm were considerably modified to adapt the structure to this new multi-band application. Therefore, this study began by evaluating the response of the newly designed reflector when combined in the laser cavity with a C-band EDFA.

As Fig. 4 shows, when this ACBFR was used as a quasi-distributed reflector under a pump power of 100 mW, a single-wavelength laser centered at 1530.84 nm with an output power level of -10 dBm was achieved. It can also be seen that an OSNR of 47 dB was reached, a value that has been demonstrated to be suitable for most of laser-sensor applications [26].

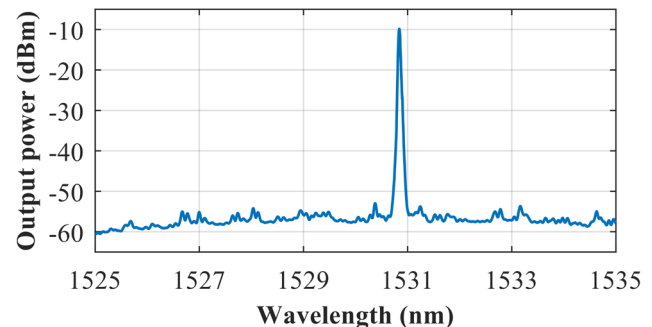


Fig. 4. Output spectra of the ring-cavity fiber laser when pumped by a 976-nm laser at 100mW while using the ACBFR, measured by an OSA.

Fig. 5 illustrates the output power level as a function of pump power for the ring-cavity fiber laser. The achieved laser presents a pump threshold of 48 mW, and an efficiency of about 0.2 %. This value of efficiency was to be expected in view of previous works [22], with respect to which the average micro-drilling pulse energy has been reduced. As a result, refractive index variations have also been smoothed to values under 10^{-3} , lowering the reflectance obtained by the quasi-distributed mirror.

> REPLACE THIS LINE WITH YOUR MANUSCRIPT ID NUMBER (DOUBLE-CLICK HERE TO EDIT) <

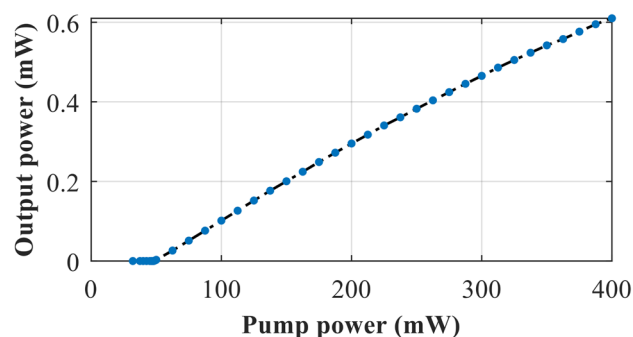
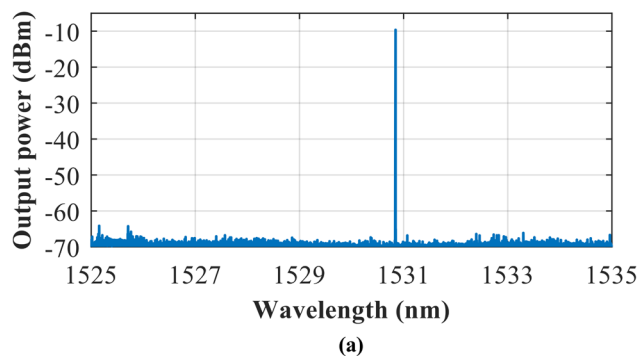
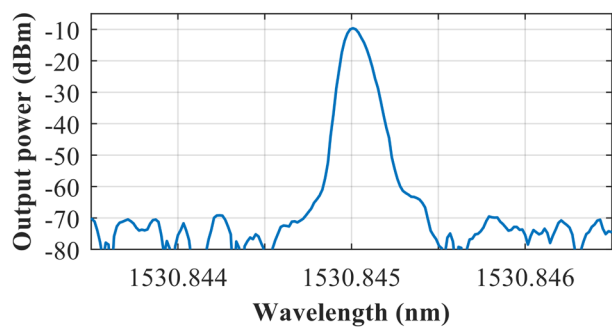


Fig. 5. Output power versus pump power for the C-band ACBFR-based fiber laser.

Following the characterization of the laser achieved, its longitudinal-modal behavior was also evaluated. For this purpose, a high-performance optical spectrum analyzer (Aragon Photonics BOSA-C) capable of providing a spectral resolution of 0.08 pm with a dynamic range greater than 80 dB was employed. Given that the total length of the cavity was short enough to fit the spectral resolution of the instrument, it was suitable to discriminate between longitudinal modes. The result of the characterization at 100 mW is shown in Fig. 6 (a) where, taking into account the previous consideration, SLM behavior could be verified. A detailed view of this output spectrum is illustrated in Fig. 6 (b).



(a)



(b)

Fig. 6. Output spectra of the ring-cavity fiber laser when pumped by a 976-nm laser at 100mW while using the ACBFR, measured by the BOSA-C (a), and its detailed view (b).

Regarding the emitted wavelength, it was constrained by the peak core gain of the I25 gain medium employed, located at around 1531 nm. This was to be expected given that the spectral response of the reflector was found to be low and reasonably flat, albeit with a slight ripple. Thus, it was the amplifier and

not the reflector that mainly imposed the wavelength of oscillation.

Finally, the output power stability over time was investigated. To this end, the peak power of the 1530.84 nm emission line was tracked for different levels of pump power up to 400 mW and during 1 hour in each case. The result achieved were instabilities under 0.08 dB for a confidence level (CL) of 95 % in all cases, reaching a minimum value of 0.04 dB when pumped at 100 mW, as shown in Fig. 7. Recently reported schemes suggest that saturable absorbers, multiple intracavity interferential filters and ultra-narrow FBGs need to be simultaneously employed to achieve a comparable level of stability [27][28]. Moreover, output power stabilities of this magnitude were only possible by means of 5 W of Raman amplification in the particular case of ACBFR-based lasers [29].

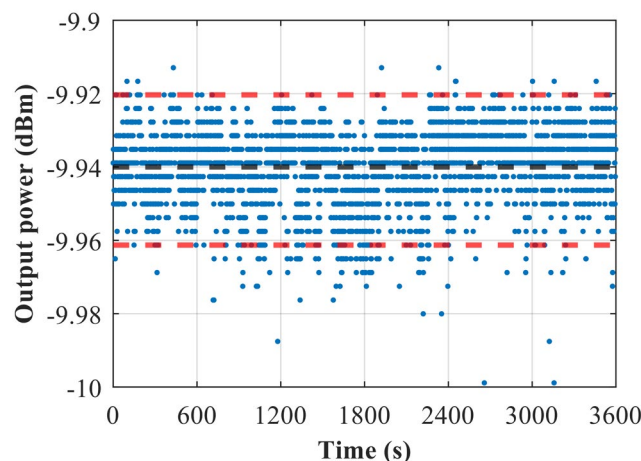


Fig. 7. Output power stability when pumped by a 976-nm laser at 100 mW and using the ACBFR, measured over 1 h with a CL of 95 %. The red dashed lines represent the confidence interval limits, while in black the mean peak power is plotted.

B. L-band Laser Generation Properties

Once the EDFA was replaced by the already mentioned L-band EDFA, the previous characterization was repeated. In this case, laser oscillation was achieved without the need for additional components. Moreover, as Fig. 8 illustrates, for the same level of pump power, similar results were obtained. In detail, a single emission line centered at 1598.80 nm with an output power level of about -10.5 dBm and an OSNR of 44 dB was achieved. These values have been proven fully suitable for most sensing applications [18], [20].

As in the previous case, the central lasing wavelength was mostly determined by the peak gain of the L-band EDFA employed, that is around 1598 nm.

After that, the output power as a function of pump power was monitored up to 400 mW. As presented in Fig. 9, the power threshold could not be reached as the minimum pumping power supported by the EDFA employed exceeds 50 mW. In any case, the 50 mW limit ensures that the L-band oscillation threshold will be at most that of the C-band, if not lower. The obtained laser efficiency was 0.08 %, less than half of the previously obtained by using the C-band amplification.

> REPLACE THIS LINE WITH YOUR MANUSCRIPT ID NUMBER (DOUBLE-CLICK HERE TO EDIT) <

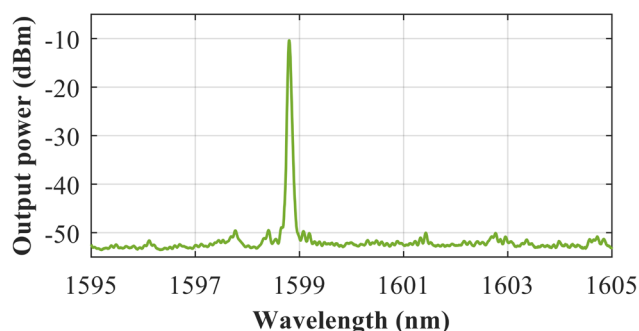


Fig. 8. Output spectra of the L-band ring-cavity fiber laser when pumped at 100mW while using the ACBFR, measured by an OSA.

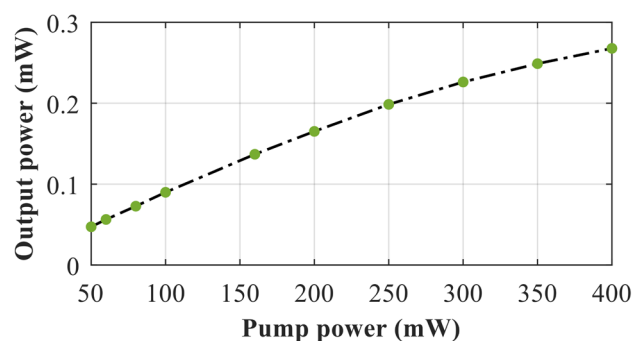


Fig. 9. Output power versus pump power for the L-band ACBFR-based fiber laser.

Given that the BOSA-C analyzer is limited to C-band, SLM operation was corroborated by conducting heterodyne detection of the output signal. For this purpose, the L-band laser line was combined with the output of a commercial tunable laser source (TLS; Agilent 8164B) by using a 3 dB optical coupler. Once the 100 KHz linewidth oscillation of the TLS was tuned close enough to 1598.80 nm, the resulting beating signal was detected after a photodetector (Optilab PD-20-M) by means of an electrical spectrum analyzer (ESA; R&S FSP30). Fig. 10 illustrates the output optical spectrum obtained, where SLM behavior is observed.

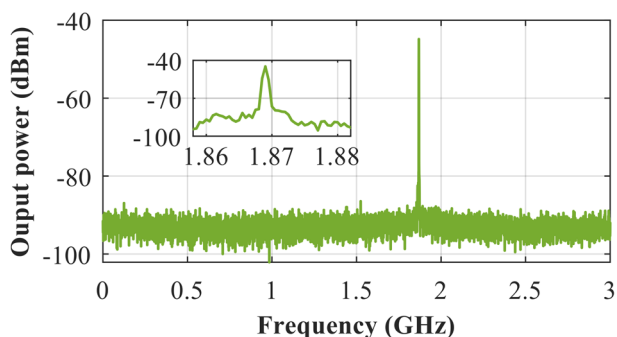


Fig. 10. Output spectra of the L-band ring-cavity fiber laser when pumped at 100 mW while using the ACBFR, measured by an ESA when a TLS was tuned close to 1598.8 nm.

L-band output power level stability over time, as a function of the injected pump power, was also evaluated. Following the procedure already introduced, pump power was steadily

increased at regular steps while monitoring the peak power of the single-wavelength laser centered at 1598.80 nm for one hour per step. The result achieved showed output power instabilities under 0.09 dB for a CL of 95 % in all cases, reaching a minimum value of 0.08 dB when pumped at 200 mW. As in the previous case, combining different intracavity filtering techniques, such as fiber Sagnac interference loop with angle shift spliced polarization maintaining fibers [30], comparable values of stability could be reached. For consistency with the study, Fig. 11 illustrates the 0.086 dB output power instability obtained when pumped at 100 mW.

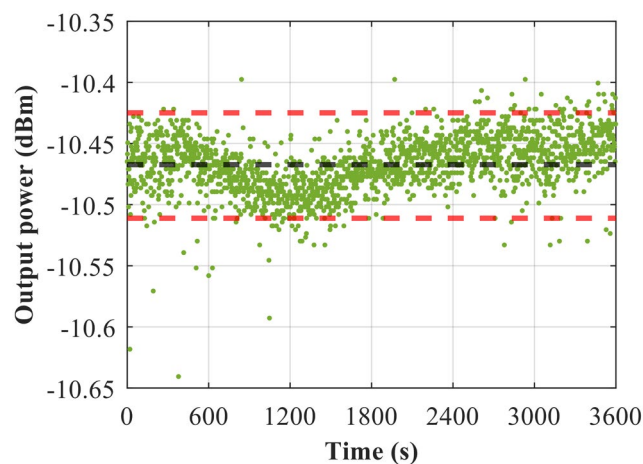


Fig. 11. Output power stability of the L-band laser when pumped at 100 mW while using the ACBFR, measured over 1 h with a CL of 95 %. Red dashed lines represent the confidence interval limits. The mean peak power is plotted in black.

Although slightly worse than the stabilities obtained in the C-band results, both cases remained well under the 0.1 dB instability threshold. Comparing with other reported optical fiber resonators for dual band sensing applications, it represents an enhancement of almost an order of magnitude [31].

C. Temperature and Strain Sensing

Next, the performance of the reflector as a temperature sensor was evaluated. For this purpose, the ACBFR was placed into a climatic chamber (BINDER FD 23). While connected to the ring-cavity fiber laser, the resonance wavelength shift was measured as the temperature was steadily increased from room-temperature to 75°C. The tracking was carried out by means of an OSA, and the measurements were performed for both C- and L-band lasers. The results are presented in Fig. 12. As can be seen, both cases show a strong linear trend with sensitivities of 9.7 and 10.2 pm/°C, for C- and L-band in that order. These results are also in agreement with previous studies and comparable to the values attained for commercial fiber Bragg gratings operating in this spectral range, which is around 11 pm/°C [25].

> REPLACE THIS LINE WITH YOUR MANUSCRIPT ID NUMBER (DOUBLE-CLICK HERE TO EDIT) <

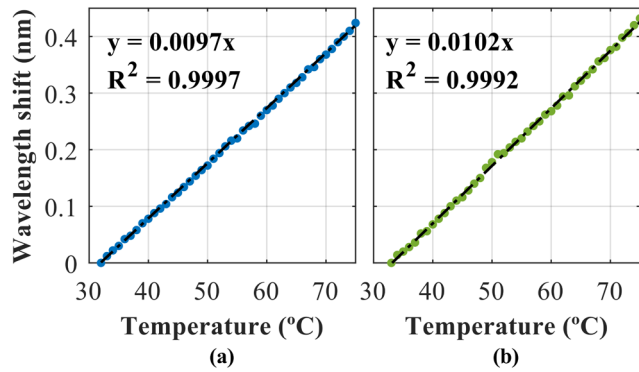


Fig. 12. Wavelength shift as function of temperature when using the ACBFR for the C-band laser (a), and L-band laser (b).

Finally, the reflector was introduced into a custom-built station designed for strain measurements. Here, two motorized clamps allow the tensioning of the FUT. The distances between them are adjusted and the positioning error is dynamically corrected down to 17 nm, achieving a final resolution of $0.09\mu\epsilon$. As in the previous case, the tracking of the central emission wavelength was performed by means of an OSA, and its shift was characterized both for C- and L-band lasers. As a result, Fig. 13 shows a linear dependency of the wavelength shift on the applied strain, reaching sensitivities of 10.4 and 10.7 pm/ $\mu\epsilon$ respectively. Both values represent a substantial enhancement of the sensitivity achieved with respect to classical structures, exceeding that of FBGs by up to one order of magnitude [32].

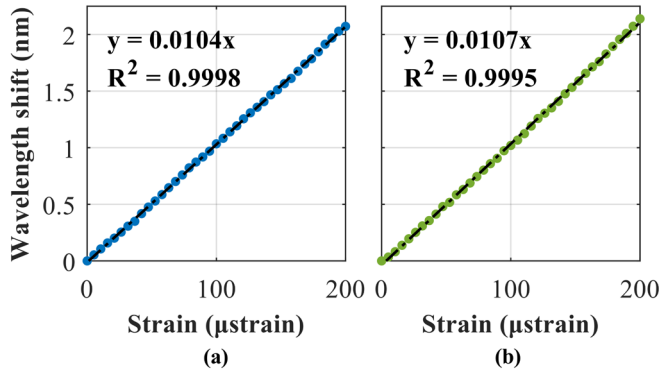


Fig. 13. Wavelength shift as function of the strain applied to the ACBFR for the C-band laser (a), and L-band laser (b).

Thus, it has been shown that this new type of structure allows fiber laser sensing systems for both temperature and strain measurements with comparable (temperature) or greater (strain) sensitivities than those based on classical fiber mirrors, such as FBGs. Furthermore, the operating wavelength is mainly determined by the optical amplifier employed in the system and no longer by the reflector itself. Herein lies the real improvement, as it allows high-performance multi-band sensors to be attained without higher costs or a more complex manufacturing process than that of other classical reflectors for sensing.

V. CONCLUSIONS

This work presents an experimental analysis and comparison of the performance attained by an artificially controlled backscattering fiber reflector when employed in a ring resonator for C- and L-bands fiber lasers. Following the switchable behavior already noted in previous works [15], the first goal of the research has been to demonstrate the feasibility of achieving ultra-stable oscillation regardless of the optical band under study if assisted by this type of reflectors. To this end, a new kind of ACBFR has been designed and inscribed. Once introduced in a ring resonator as a quasi-distributed reflector, laser emission has been achieved for a pump threshold below 50 mW in both amplification bands. Moreover, single-longitudinal mode operation for pumps over 100 mW has been attained with either amplifier, with OSNRs higher than 44 dB and output power level instabilities between 0.04 and 0.09 dB. In this regard, it can be stated that the use of an ACBFR has made it possible to obtain longitudinal single-mode operation, providing stability to the laser performance. It has also been noted that the emission line falls in the vicinity of the amplified spontaneous emission peak, supporting the assumption that the lasing wavelength is mainly determined by the optical amplifier employed and not only by the micro-drilled structure designed. Finally, its performance as a fiber laser sensing system for temperature and strain has been evaluated, obtaining sensitivities of around 10 pm/ $^{\circ}\text{C}$ and 10.5 pm/ $\mu\epsilon$ in both cases. Relative to FBGs, the ACBFRs show an enhancement of one order of magnitude in strain sensitivity while temperature sensitivity remains comparable.

REFERENCES

- [1] G. A. Ball, W. W. Morey, and P. K. Cheo, "Single- and multipoint fiber-laser sensors," *IEEE Photon. Technol. Lett.*, vol. 5, no. 2, pp. 267-270, Feb. 1993.
- [2] L. Talaverano, S. Abad, S. Jarabo and M. Lopez-Amo, "Multiwavelength fiber laser sources with Bragg-grating sensor multiplexing capability," *J. Light. Technol.*, vol. 19, no. 4, pp. 553-558, April 2001.
- [3] X. Yang, S. Bandyopadhyay, L. Shao, D. Xiao, G. Gu, and Z. Song, "Side-polished DBR fiber laser with enhanced sensitivity for axial force and refractive index measurement," *IEEE Photon. J.*, vol. 11, no. 3, pp. 1-10, June 2019.
- [4] W. Zhang, Z. Wang, W. Huang, W. Liu, L. Li, and F. Li, "Fiber laser sensors for micro seismic monitoring," *Measurement*, vol. 79, pp. 203-210, Feb. 2016.
- [5] Y. Liang, L. Jin, L. Wang, X. Bai, L. Cheng, and B. Guan, "Fiber-laser-based ultrasound sensor for photoacoustic imaging," *Sci. Rep.*, vol. 7, 40849, Jan. 2017.
- [6] R.A. Perez-Herrera, A. Stancalie, P. Cabezudo, D. Negut, and M. Lopez-Amo, "Gamma radiation-induced effects over an optical fiber laser: towards new sensing applications," *Sensors*, vol. 20, no. 11, 3017, May 2020.
- [7] A. Bellemare, "Continuous-wave silica-based erbium-doped fibre lasers," *Prog. Quantum Electron.*, vol. 27, no. 4, pp. 211-266, April 2003.
- [8] M. Svalgaard and S. L. Gilbert, "Stability of short, single-mode erbium-doped fiber lasers," *Appl. Opt.*, vol. 36, no. 21, pp. 4999-5009, 1997.
- [9] S.K. Turitsyn, S.A. Babin, D.V. Churkin, I.D. Vatnik, M. Nikulin, and E.V. Podivilov, "Random distributed feedback fibre lasers," *Phys. Rep.*, vol. 542, no. 2, pp. 133-193, Sept. 2014.
- [10] M. Bravo, M. Fernandez-Vallejo, and M. Lopez-Amo, "Internal modulation of a random fiber laser," *Opt. Lett.*, vol. 38, no. 9, pp. 1542-1544, May. 2013.
- [11] D. Leandro, V. deMiguel, R. A. Perez-Herrera, M. Bravo, and M. Lopez-Amo, "Random DFB fiber laser for remote (200 km) sensor monitoring using hybrid WDM/TDM," *J. Light. Technol.*, vol. 34, no. 19, pp. 4430-4436, Oct. 2016.

> REPLACE THIS LINE WITH YOUR MANUSCRIPT ID NUMBER (DOUBLE-CLICK HERE TO EDIT) <

- [12] L. Rodriguez-Cobo, R. A. Perez-Herrera, M. A. Quintela, R. Ruiz-Lombera, M. Lopez-Amo, and J. M. Lopez-Higuera, "Virtual FBGs using saturable absorbers for sensing with fiber lasers," *Sensors*, vol. 18, no. 11, 3593, Oct. 2018.
- [13] D. Leandro, R. A. Perez-Herrera, I. Iturri, and M. Lopez-Amo. "Experimental study of the SLM behavior and remote sensing applications of a multi-wavelength fiber laser topology based on DWDMs," *Appl. Phys. B*, vol. 118, pp. 497–503, Feb. 2015.
- [14] S. Rota-Rodrigo, L. Rodriguez-Cobo, M. A. Quintela, J. M. Lopez-Higuera, and M. Lopez-Amo, "Dual-wavelength single-longitudinal mode fiber laser using phase-shift Bragg gratings," *IEEE J. Sel. Top. Quantum Electron.*, vol. 20, no. 5, pp. 161-165, Sept.-Oct. 2014.
- [15] R. A. Perez-Herrera, P. Roldan-Varona, L. R. Cobo, J. M. Lopez-Higuera, and M. Lopez-Amo, "Single longitudinal mode lasers by using artificially controlled backscattering erbium doped fibers," *IEEE Access*, vol. 9, pp. 27428-27433, Feb. 2021.
- [16] L. Yu, T. Liu, K. Liu, J. Jiang, L. Zhang, Y. Jia, and T. Wang, "Development of an intra-cavity gas detection system based on L-band erbium-doped fiber ring laser," *Sens. Actuator B-Chem.*, vol. 193, pp. 356-362, Mar. 2014.
- [17] W. Li, A. Zhang, Q. Cheng, C. Sun, and Y. Li, "Theoretical analysis on SPR based optical fiber refractive index sensor with resonance wavelength covering communication C+L band," *Optik*, vol. 213, 164696, July 2020.
- [18] R. A. Perez-Herrera, A. Ullan, D. Leandro, M. Fernandez-Vallejo, M. A. Quintela, A. Loayssa, J. M. Lopez-Higuera, and M. Lopez-Amo, "L-band multiwavelength single-longitudinal mode fiber laser for sensing applications," *J. Light. Technol.*, vol. 30, no. 8, pp. 1173-1177, Mar. 2012.
- [19] T. Miya, Y. Terunuma, T. Hosaka, and T. Miyashita, "Ultimate low-loss single-mode fibre at 1.55 μm ," *Electron. Lett.*, vol. 15, no. 4, pp. 106-108, Feb. 1979.
- [20] J. Marshall, G. Stewart, and G. Whitenett, "Design of a tunable L-band multi-wavelength laser system for application to gas spectroscopy," *Meas. Sci. Technol.*, vol. 17, no. 5, pp. 1023–1031, Apr. 2006.
- [21] P. Roldan-Varona, D. Pallares-Aldeiturriaga, L. Rodriguez-Cobo, and J. M. Lopez-Higuera, "Slit beam shaping technique for femtosecond laser inscription of enhanced plane-by-plane FBGs," *J. Light. Technol.*, vol. 38, no. 16, pp. 4526-4532, Aug. 2020.
- [22] R. A. Perez-Herrera, D. Pallares-Aldeiturriaga, A. Judez, L. Rodriguez-Cobo, M. Lopez-Amo, and J. M. Lopez-Higuera, "Optical fiber lasers assisted by microdrilled optical fiber tapers," *Opt. Lett.*, vol. 44, no. 11, pp. 2669-2672, May 2019.
- [23] R. A. Perez-Herrera, A. Stancalie, P. Cabezudo, D. Sporea, D. Neguț, and M. Lopez-Amo, "Gamma radiation measurements using an optical fiber laser," in *Proc. 26th Int. Conf. Optical Fiber Sensors*, Lausanne, Switzerland, Sept. 2018, WF37.
- [24] R. A. Pérez-Herrera, M. A. Quintela, M. Fernández-Vallejo, A. Quintela, M. López-Amo, and J. M. López-Higuera, "Stability comparison of two ring resonator structures for multiwavelength fiber lasers using highly doped Er-fibers," *J. Light. Technol.*, vol. 27, no. 14, pp. 2563-2569, July 2009.
- [25] R. A. Perez-Herrera, M. Bravo, P. Roldan-Varona, D. Leandro, L. Rodriguez-Cobo, J. M. Lopez-Higuera, and M. Lopez-Amo "Micro-drilled optical fiber for enhanced laser strain sensors," in *Proc. 7th European Workshop on Optical Fibre Sensors*, Limassol, Cyprus, Aug. 2019, vol. 11199, 111992R
- [26] S. Pevec, and D. Donlagic, "Multiparameter fiber-optic sensors: a review," *Opt. Eng.*, vol. 58, no. 7, 072009, Mar. 2019.
- [27] T. Feng, F. Yan, W. Peng, S. Liu, S. Tan, X. Liang, and X. Wen, "A high stability wavelength-tunable narrow-linewidth and single-polarization erbium-doped fiber laser using a compound-cavity structure," *Laser Phys. Lett.*, vol. 11, no. 4, 045101, Feb. 2014.
- [28] Z. Wang, J. Shang, K. Mu, S. Yu and Y. Qiao, "Stable single-longitudinal-mode fiber laser with ultra-narrow linewidth based on convex-shaped fiber ring and Sagnac loop," *IEEE Access*, vol. 7, pp. 166398-166403, Nov. 2019.
- [29] R. A. Perez-Herrera, P. Roldan-Varona, M. Galarza, S. Sañudo-Lasagabaster, L. Rodriguez-Cobo, J. M. Lopez-Higuera, and M. Lopez-Amo, "Hybrid Raman-erbium random fiber laser with a half open cavity assisted by artificially controlled backscattering fiber reflectors," *Sci. Rep.*, vol. 11, 9169, Apr. 2021.
- [30] Z. Ding, Z. Wang, C. Zhao, and D. Wang, "Tunable erbium-doper fiber laser based on optical fiber Sagnac interference loop with angel shift spliced polarization maintaining fiber," *Opt. Fiber Technol.*, vol. 42, pp. 1-5, May 2018.
- [31] Y. Zhou, S. Lou, Z. Tang, T. Zhao, and W. Zhang, "Tunable and switchable C-band and L-band multi-wavelength erbium-doped fiber laser employing a large-core fiber filter," *Optics & Laser Technol.*, vol. 111, pp. 262-270, Apr. 2019.
- [32] C. E. Campanella, A. Cuccovillo, C. Campanella, A. Yurt, and V. Passaro, "Fibre Bragg grating based strain sensors: review of technology and applications," *Sensors*, vol. 18, no. 9, 3115, Sept. 2018.